ELSEVIER

Marine Geology 160 (1999) 147–170

MARINE GEOLOGY
INTERNATIONAL JOURNAL OF MARINE GEOLOGY, GEOCHEMISTRY AND GEOPHYSICS

www.elsevier.nl/locate/margeo

A laboratory examination of floc characteristics with regard to turbulent shearing

A.J. Manning *, K.R. Dyer

Institute of Marine Studies, University of Plymouth, Drake Circus, Plymouth, PL4 8AA, UK

Received 31 October 1997; accepted 15 January 1999

Abstract

Turbulent shear generated within the water column is recognised as having a controlling influence over both the flocculation of fine grained cohesive sediments within estuarine waters, and their respective aggregate break-up. This study examines the inter-relationships between floc characteristics over increasing turbidity (80–200 mg l^{-1}) and turbulent shear (0–0.6 N m^{-2}) environments, by the use of a laboratory flume within which a suspension can be sheared at a controlled rate, and with an unintrusive macro-lens miniature video camera mounted in a viewing port on the flume channel wall. The camera enables the direct simultaneous measurement of both floc size and settling velocity, from which accurate estimates of floc effective density and porosity can be made. Measurements were made 120 s after the induced turbulence has ceased. The instrument has an upper viewing turbidity limit of 210 mg l^{-1}, and a lower resolution of 20 μm. The sediment was collected from the inter-tidal mudflats at Weir Quay on the Tamar Estuary in Devon, Southwest England. The results indicated that increasing turbidity at low shear levels encouraged floc growth, but the effect of the increasing turbulent shear (0.35 N m^{-2}) together with increasing concentration in suspension causes disruption rather than enhancing the flocculation process. At shears up to 0.35 N m^{-2}, the largest size and settling velocity flocs were produced at high concentrations, whereas above 0.35 N m^{-2} disruption caused smaller flocs at higher concentrations. The use of algorithms which were based either on a single floc characteristic (i.e., size or settling velocity) or a mean fractal dimension, were seen not to accurately approximate the experimental data. A multiple regression analysis of the experimental data produced the following formula, based on mean values of the 20 largest flocs sampled under each of the imposed environmental conditions (referred to as max20size mean values): settling velocity = 0.301 − 0.00337 rms of the gradient in turbulent velocity fluctuations − 0.000606 SPM + 0.00335 floc size, which proved to be the most accurate representation with an R^2 value of 0.95. A similar formula was determined for the average value of the four fastest settling flocs within each sample-group (max4W_S). This highlights the importance of modelling algorithms that are developed from data that take into account effective density variations (i.e., simultaneous size and settling velocity measurement).

Keywords: floc size; turbulent shear; settling velocity; effective density; flocculation

* Corresponding author. Fax: +44-1752-232-406; E-mail: amanning@plymouth.ac.uk

PII: S0025-3227(99)00013-4

1. Introduction

The ability to predict the sediment transport regime within near-shore waters is of significant economical and environmental importance. When predicting both mass settling flux and deposition rates, the settling speed of the suspended matter is a key parameter. Settling velocities are a function of particle size and density, but this is complicated within an estuarine environment by suspended particulate matter (SPM) flocculation to form aggregates, or flocs, which are larger but less dense than the individual primary particles. An individual floc may constitute up to 10^6 individual particles. This means that there is the possibility of particles ranging over four orders of magnitude, from clay particles of 1 μm to flocs of several centimetres, and the settling velocities also ranging over four orders of magnitude, from 0.01 mm s^{-1} up to several centimetres per second (Lick, 1994). To further complicate matters, flocculation is a dynamically active process which is directly affected by its environmental conditions; this results in a continual process of aggregation and disaggregation, and hence a continual change in floc properties.

Until recently, studies on flocculation established general power relationships between floc settling velocity and turbidity (Dyer, 1986); and floc size and settling velocity (Gibbs, 1985) and these formulae have been applied within estuarine hydro-dynamical modelling. Also, in order for the floc characteristics of those formed either in situ or within a laboratory flume to be measured, the aggregates have to be initially sampled by a device such as a Niskin bottle (Gibbs and Konwar, 1983) or pipettes, or the Owen Tube (Owen, 1971), but all these techniques are very disruptive (Gibbs, 1985; Van Leussen, 1988). This could account for the reason that previous studies tended to show a much lower floc size range than is now known.

The presence of large estuarine macro flocs has been observed by in situ photography (Eisma et al., 1983, 1990), and laser particle sizer measurements (Bale and Morris, 1987), but these provided no indication of settling velocity. Most instruments measured either size or settling velocity, and use Stokes' Law to predict the non-measured characteristic; this required making an assumption of the floc effective density (also known as density contrast, density difference or excess density). However, the settling velocity of a floc is the function of both floc size and the respective effective density.

Very few quantitative studies have been conducted on floc effective density variations. Direct analysis by settling flocs in sucrose solutions are suspect, in that, even if the aggregates survive the sampling process, the floc porewater may be replaced by the sucrose solution. The advent of in situ video camera systems (Van Leussen and Cornelisse, 1994; Fennessy et al., 1994a), has permitted both floc size and settling velocity to be established simultaneously, with the opportunity to estimate effective density via Stokes' Law.

A knowledge of effective density, ρ_e, is important in the calculation of the vertical settling fluxes since the majority of the mass is in the low density, high settling velocity, large flocs (Mehta and Lott, 1987). Also, the rheological properties of SPM are governed by volume concentrations, as opposed to mass concentrations (Dyer, 1989). Fennessy et al. (1997) explains a technique by which the floc population samples obtained by the INSSEV (In Situ Settling Velocity) instrument (Fennessy et al., 1994a) could be processed into settling flux spectra. Utilising this spectral technique, a number of field experiments were conducted within the Tamar estuary, South West England (Fennessy, 1994) and the Elbe estuary, North West Germany (Fennessy and Dyer, 1996), and they both identified the larger macro flocs containing the majority of the mass flux. This finding concurs with a hypothesis offered by Eisma et al. (1990).

One factor that has been greatly overlooked is the quantitative effect turbulence has on the flocculation process. In estuaries, turbulent shear within the water column causes particulates to collide, and this can result in strongly bonded, orthokinetically-formed, aggregates. As the flocs settle through the water column, many authors such as Van Leussen (1994), and Lick et al. (1993) have attributed the collision mechanism of differential settling as having a major influence on further floc growth. However, Stolzenbach and Elimelich (1994) have suggested that differential settling is not an important factor.

The velocity gradients are largest in the near bed region (10–20% of the water column depth), and

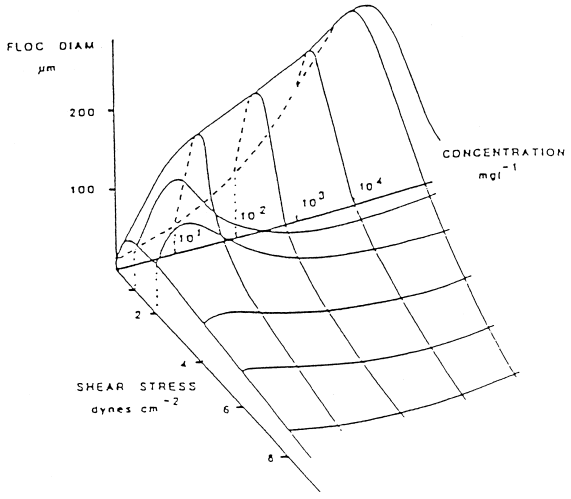

Fig. 1. Conceptual diagram illustrating the relationship between floc size, shear stress and suspended sediment concentration (from Dyer, 1989).

approximately 80% of the turbulent energy generated by the water flow occurs within this zone. There the strongest lift and shear forces occur, controlling the maximum size of the suspended flocs (Mehta and Partheniades, 1975). Only flocs that have a strength that exceeds those of the shearing forces will settle to the bed. The weaker flocs are broken up, primarily as a result of three-particle contact (Burban et al., 1989), into either smaller flocs or individual particles, and re-entrained. So, under the influence of turbulent forces there is a continuous process of flocculation and break-up, resulting in a dynamic equilibrium of the flocs (strength, size and density) within a given shear field.

Also, the presence of increasing levels of SPM, can provide the potential for an increase in inter-particle contacts. Studies by Eisma et al. (1991), from measurements taken in a variety of West European estuaries, showed that the floc size tended to be larger near the bottom (at 10–15% of the water depth) than at the surface. They explained this by suggesting that the increase in SPM concentration was having the effect of reducing turbulence, therefore increasing the frequency of particle collisions, and hence causing enhanced flocculation.

Burban et al. (1989) conducted an investigation on the interactive effects of shear, SPM concentration and salinity, with respect to floc diameter. This was then extended to include settling velocity (Burban et al., 1990). However, these laboratory experiments relied on withdrawing floc samples formed within a flocculator at a constant shear level, and then transplanting them into a settling tube for measurement. Even so, Burban (1987) and Tsai et al. (1987) both indicated, from laboratory experiments, that the modal floc size was influenced by both the SPM concentration and shear stress. A conceptual model illustrating expected trends (Fig. 1), was proposed by Dyer (1989). Even so, relatively little quantitative data has been obtained on these inter-relationships. The purpose of this study was to use current unintrusive video camera technology in a laboratory flume, under varying controlled levels of both SPM concentrations and turbulent shear, to determine flocculated aggregate characteristics. The instrument involved an annular flume containing suspensions with concentrations up to 200 mg l^{-1}, sheared at rates up to 0.6 N m^{-2}. The floc size and settling velocities were measured using a video camera, and effective densities were calculated by Stokes' Law. This quantitative technique is compared with a number of the modelling algorithm approaches that are initially summarised in the following section.

2. Modelling approaches

Various mathematical models have been proposed on flocculation under turbulent conditions. Early

studies by Argaman and Kaufman (1970) and Parker et al. (1972) derived a model that simultaneously examined the flocculation response to turbulence-induced growth and break-up. The formulae included many parameters that were difficult to measure, and Ayesa et al. (1992) later formulated a calibration algorithm for the model, based on experimental results using varying particulate suspension levels. However, this still provided little information about the settling characteristics of the aggregates predicted.

More recently, a number of authors have proposed simple formulae inter-relating a number of floc characteristics which can then be calibrated by empirical study. Such an approach has been used by Van Leussen (1994), who has utilised a formula which modifies the settling velocity in still water, by a growth factor due to turbulence divided by a turbulent disruption factor:

$$W_S = W_{S0}\frac{1+aG}{1+bG^2} \tag{1}$$

where W_S is settling velocity, G is the root mean square of the gradient in turbulent velocity fluctuations, a and b are empirically determined constants. Eq. (1) was initially proposed by Argaman and Kaufman (1970), and it is a simplification of their original formulation. The reference settling velocity (taken at zero turbulence), W_{S0}, is related to the SPM concentration (C) by:

$$W_{S0} = kC^m \tag{2}$$

where k is an empirical constant, and m is the exponent. Eq. (1) is a qualitative simplification of the Argaman and Kaufman model, with only a limited number of inter-related parameters, and hence does not provide a complete description of floc characteristics within a particular shear environment.

Lick et al. (1993) similarly derived an empirical relationship where floc diameter (D_X) was found to vary as a function of the product of the SPM concentration and turbulent shear (in s^{-1}), where c and d are empirically determined values:

$$D_X = c(\mathrm{SPM}\,G)^{-d} \tag{3}$$

A more complex model has been proposed by Winterwerp (1997). This was based on Kranenburg (1994), who made the assumption that flocculated mud could be represented by a self-similar fractal structure. This is the same as the order of aggregation theory, suggested by Krone (1963, 1986) and Partheniades (1965); i.e., primary particles together form zero order flocs, these in turn combine to form 1st order flocs, etc. Primary particles of diameter D_p, are related to the floc size D_f as follows:

$$N \sim \left[D_f/D_p\right]^{nf} \tag{4}$$

where N is the total number of particles in the fractal aggregate, and nf is the fractal dimension:

$$nf = \ln m_1/\ln m_2 \tag{5}$$

where m_1 is the number of primary particles to form a first order floc; m_2 is a factor by which the floc will increase in size during this hierarchical process (i.e., the number of primary particles of the second order floc formed). From this, Kranenburg derived that:

$$(\rho_f - \rho_w) \sim (\rho_{sed} - \rho_w)\left[D_p/D_f\right]^{3-nf} \tag{6}$$

with ρ_f representing the floc bulk density, ρ_{sed} and ρ_w the sediment and water density, respectively. Substituting Eq. (6) into the classic Stokes' equation, Winterwerp (and similarly Tambo and Watanabe, 1979) obtained the following relationship:

$$W_S = \alpha' D_p^{3-nf}\left[(\rho_{sed} - \rho_w)\,g\right]/\mu\, D_f^{nf-1} \tag{7}$$

where α' is an empirically-derived constant, and μ is viscosity. Eqs. (6) and (7) were substituted into a simple aggregation and break-up formula based on G, as the turbulence factor, to provide a linear combination of the processes. Values for the fractal dimension generally range between 1.4 (for fragile flocs) and 2.5 (for strong estuarine flocs). However, in order to make the model solvable analytically, an average nf value has to be used. So using data by, among others, Gibbs (1985), Van Leussen (1994), and Fennessy et al. (1994a), a linear regression revealed an average nf of 2.

Another model, proposed by Hill (1996), uses sectional and discrete representations based on the Pandya and Spielman (1982) statistical population-

balance approach to floc breakage, which was then incorporated into commonly used particle-aggregation models. Similar to the Winterwerp model, this approach treats the flocs as fractal objects, and hence requires an average fractal dimension value.

However, initial video camera field studies of flocculation characteristics over a tidal cycle by Fennessy et al. (1994b), revealed significant variations in floc effective density, so the applicability of an average fractal dimension, and the empirical approach offered by Lick et al. (1993), will each be examined later in this paper.

3. Instrumentation

In order to satisfy the study objectives, the instrumentation had to be able to accurately shear a sediment concentration to a required level on a repeatable basis, whilst also permitting the measurement of the characteristics demonstrated by the fragile flocs formed under the imposed environment.

3.1. Annular flume

The design incorporated an annular flume, filled with a pre-determined SPM concentration with an underwater video camera. This aggregate suspension could then be sheared for a set duration at a desired level to obtain equilibrium floc sizes. The floc aggregates could be viewed via the video camera mounted externally on the outer wall of the flume, and the recorded images used to calculate the floc characteristics.

The annular flume has an outer diameter of 1.2 m, a channel width of 0.10 m and a depth of 0.15 m, along with a detachable roof 10 mm thick. The flume channel is constructed of fibreglass with a rotating roof section. An adjustable annular ring, which has six 15 mm deep wooden paddles on the underside, was suspended from the roof. The annular ring fits into the channel, and is set to the height of the fluid. As the annular ring rotates, motion in the flume is induced by the drag between the ring and the fluid surface.

The roof is driven by an electronic torque stepper motor, that is computer-controlled. The speed of the motor, and hence the roof speed, is input via a micro computer and custom written software supplied by Valeport. The stepper motor produces a maximum speed of 1 m/s at the centre of the channel.

3.2. Video camera system

The video camera is a high resolution monochrome Pasecon tube model, with built-in integral low heat illumination (supplied by Custom Camera Designs of Wells, England), similar to that used in the INSSEV instrument (Fennessy et al., 1994a). It has a back-illumination system in which particles appear dark on a light background (i.e., a silhouetting technique); this reduces image smearing, and makes the floc structure more clearly visible. As concentration levels increase within the water column, an auto-gain LED annulus compensates so as to produce a clear video image of the flocs. The camera and video recorder combination has a practical lower limit of resolution of 20 μm.

The camera lens fits flush with the channel wall and is in direct contact with the water via a viewing port. The system is set to focus on particles 45 mm from the camera lens, and to ensure that all particles viewed are the same distance from the camera (and to reduce the likelihood of overlapping floc images), it exhibits a 1 mm depth of field. The viewing height was 93 mm below the surface of the water column (i.e., 42 mm above the flume base), and in the centre of the channel.

4. System calibration

Initial testing revealed that the video system had a maximum operational turbidity level of 210 mg l^{-1} (Manning, 1996). This was because, unlike the INSSEV instrument (Fennessy et al., 1994a), the flume system cannot selectively reduce the number of flocs which are viewed by the video camera as the turbidity increases. Prior to experimental use, the flume had to be calibrated, and this procedure is separated into two distinct aspects.

4.1. Turbulent shear stress

It was not possible to measure the entire velocity profile within the flume channel, so the average

turbulent shear stress values were determined within the flume. This was achieved by measuring the average flow velocity using a miniature Nixon Streamflow impeller flow meter. The flow meter was inserted through the side wall of the annular flume via a water tight gasket; this allowed the probe to be moved across the entire width of the channel. It was also positioned at the height coincident to that of the video camera viewing axis for the experimental study (42 mm above the channel base).

The annular ring was then rotated at varying speed increments. At each rotational speed, the flow meter measured the water velocity at 10 mm intervals across the width of the channel. From this, the mean flow velocity u across the channel was determined. The frictional (shear) velocity U^* was then calculated by (Delo, 1988):

$$U_* = u n g^{-1} / h^{1/6} \quad (8)$$

where n is Manning's bed roughness coefficient, g is acceleration due to gravity, and h is the depth of flow. The flume had a very smooth channel surface, and a Manning roughness coefficient of 0.011 (Chow, 1959) was estimated. The average shear stress (τ) was then calculated as:

$$\tau = \rho_w U_*^2 \quad (9)$$

To enable an inter-comparison with previous studies, the bed shear stress values computed for the flume were converted into two commonly used alternatives (Van Leussen, 1994). The first is, the root mean square of the gradient in turbulent velocity fluctuations (G), with the units of s^{-1}:

$$G = U_* (u/\upsilon \cdot H)^{0.5} \quad (10)$$

where H is the water column depth, υ is the kinematic viscosity (molecular viscosity divided by the density of water), U_* and u are the frictional and mean flow velocities, respectively. The second classifies the turbulence level by the size of the dissipating eddies as defined by Kolmogorov (1941a,b), and referred to as the microscale of turbulence η (units are metres):

$$\eta = (\upsilon/G)^{0.5} \quad (11)$$

Table 1
A summary of the three turbulent shear format values

N/m^2	0.1	0.2	0.3	0.4	0.5	0.6
G (s^{-1})	12.8	18.2	24.2	30.7	37.8	45.2
η (μm)	280	234	203	180	162	148

A summary of the turbulent shear forms used is shown in Table 1.

The production of an average shear parameter means that absolute values measured, such as floc size, are dependant on the assumptions previously stated. However, the relative values are far more precise. For these reasons, the floc sizes should be regarded as typical values, rather than exact values. The calibration was carried out in clear freshwater.

4.2. Video image instrumentation

In order to calibrate the video monitor, a scale ruler was placed in the water in front of the camera lens, and both the vertical and horizontal dimensions of the screen were measured. The alignment of the camera axis to that of the flume channel was determined by suspending a fine nylon plumbline in front of the camera lens (when the flume channel was empty) and recording the image. This enabled corrections to be made to calculated settling velocities, so as to compensate for slight misalignments of the video camera to the viewed flocs. Alignment checks and operation of the video camera are discussed in more detail in Manning and Fennessy (1997).

5. Experimental method

The experimental programme had four runs with the flume containing turbidity levels of 80, 120, 160 and 200 mg l^{-1}. Prior to each experimental run, the flume channel was filled to a depth of 135 mm with a slurry consisting of the pre-determined SPM concentration specific to that individual run, together with water of a salinity of 10 [1] (an allowable deviation of ± 0.5). Water temperature was kept at 20°C

[1] Although all the salinity values are in parts per thousand, it is our protocol not to include any unit suffix.

(± 0.5°C) by accurate temperature control within the laboratory.

An individual run consisted of attaching the flume roof/annular ring section, and then activating the computer controlled stepper motor at a speed that produced a shear stress of 0.6 N m^{-2}. The annular ring was rotated for a duration of 30 min, so the flocs formed within the flume would be in equilibrium with the induced fluid shear stress. On terminating the stepper motor, the video recorder recorded the floc images seen by the camera for a period of 12 min. The flocs were seen crossing the screen at increasingly oblique angles as the flow speed decreased. The vertical component of the movement gave the settling velocity. The procedure was then repeated five times, working down to a minimum shear stress of 0.1 N m^{-2} at 0.1 N m^{-2} increments, each time allowing 30 min for the flocs to equilibrate to the new shear level. This system of starting a run at the highest shear level and then progressively reducing the rate was employed to emulate turbulent shear effects experienced in a natural marine environment; i.e., aggregates that form under high turbulent shear conditions retain this history (e.g., strong orthokinetic-bonded flocs) as they are transported to less turbulent zones within the water column where they flocculate further. During each run pipette samples were taken at camera viewing depth to provide a check on the suspension concentration.

To approximate zero shear conditions, a 0.4 m (outer perimeter) long section of the flume channel was enclosed at both ends, with the video camera viewing at the mid-point. This enclosed section of the flume channel was filled with slurries of each of the four individual SPM concentrations (used previously) in turn, and then allowed just to settle. However, because of the different experimental conditions, these results are presented for wider consideration, but not included in the detailed analysis.

The flocculation time, T_F, for each concentration and shear level was calculated using the following formula offered by Van Leussen (1994):

$$T_F = [2.306\pi]/[4\alpha\phi(10 + G)] \quad (12)$$

Where α is a cohesion collision efficiency factor and ϕ is the total volume of sediment per unit volume. Van Leussen defines the flocculation time as the time over which the number of particles in a suspension diminish to 10% as a result of flocculation. It was not possible to make physical measurements of the cohesion collision efficiency factor for the Tamar estuary mud suspension, so an estimate has been made based on the sediment mineralogy. Fitzpatrick (1991) found Tamar estuary mud to be generally high in kaolinite (primarily a result of extensive china clay quarrying within the catchment area), together with the presence of both illite and montmorillonite. Gibbs (1983) conducted experiments which measured the collision efficiency of various clay mineral suspensions at differing salinities; so based on Gibbs' study, α was estimated to be 0.163 for this experimental work. Therefore, the experimental conditions requiring the longest duration to achieve equilibrium would be for a turbulent energy dissipation rate (G) of 12.8 s^{-1}, and SPM of 80 mg l^{-1}; this resulted in a flocculation time of 27.8 min. Therefore, all samples sheared within the flume were deemed to be in equilibrium with the resultant turbulent environment.

5.1. Details of sediment tested

The test mud was obtained at low water from the inter-tidal mud flats at Weir Quay, which is 15 km upstream from the mouth of the Tamar Estuary in Devon. Previous studies have shown the mud flats at this location to be accreting at a fast rate.

For the tests, the fraction of sediment which passed through a 63 μm British Standard sieve (four on the phi scale), as a result of wet sieving, was used. This removed coarse particles leaving the finer material that generally accounted for 70–75% of the total weight of the sample. Six litres of mud supply with a concentration of 214 g l^{-1} was produced, and this was then proportionally diluted with water of salinity 10, to provide the experimental suspensions. Between experimental tests, the sediment supply was stored in a tightly sealed plastic container at a refrigerated temperature of 4°C.

6. Data analysis

Floc sizes and settling velocities were both measured directly from the video monitor display (manu-

ally), and these were then converted into the actual dimensions determined by the initial video image calibration. The flocs were measured for their dimensions both along the axis in the direction of settling (D_Y), i.e., along the direction of resultant motion, and the axis normal to it (D_X) from which a height:width ratio could be determined. However, to enable data inter-comparisons, the D_X value is generally used in this paper to compare with customary definitions, unless otherwise stated. It is assumed that the floc depth dimension D_Z is equal to D_X.

For all runs, the initial floc measurements were taken 120 s after the termination of the driving rotation producing the flow. This length of time allowed decay of the turbulence and permitted accurate measurements of aggregate settling velocities, whilst the floc characteristics were unaffected by aggregation and were still representative of the imposed level of shear stress. Further measurements were taken at both 6 and 11 min time increments. At each sampling stage, only the 20 largest flocs that came into focus were selected for size analysis, as being representative of the majority of the mass in suspension. The necessity for manual analysis of the results precluded a greater number being used. This decision was justified, since the larger flocs have the main influence on the mass settling flux within an estuary (Eisma et al., 1990).

The settling velocity was obtained as the vertical component of the resultant velocity, the time being provided by the frame counter also recorded on the video tape (one frame = 0.04 s). These values were then multiplied by a factor of 1.03 (Allen, 1975), to compensate for the drag due to the flume walls. To reduce the effect of secondary currents affecting the settling velocities, the flocs were measured at a mid-channel position. The video tape analysis did not reveal signs of any significant secondary circulation, e.g., wave-like images on the video monitor display. Also the flocs were settling consistently; all within clear focus by the camera. If they were going from in to out of focus during settling, this would indicate they were being influenced by secondary flows. Backtracking calculations of each individual floc sampled at all three time intervals also suggested that residual turbulence within the water column had a negligible influence on the respective settling velocities measured.

The effective density was calculated for each floc using the measured size and settling velocity using Stokes' Law:

$$W_S = \frac{D_Y D_X (\rho_f - \rho_w) g}{18 \mu} \tag{13}$$

where W_S is the settling velocity, D_X is the horizontal floc diameter, D_Y is vertical floc diameter, g is gravity, and μ is the dynamic molecular viscosity. Although Gibbs (1985) and Alldredge and Gotschalk (1988) have shown that flocs with height:width ratios of up to 1.6:1 can produce a settling factor similar to that of a perfect sphere, the modified version of Stokes law which assumes the flocs to be ellipsoidal in shape was used. This was principally to reduce inconsistencies that developed when using the spherical assumption, particularly in the floc dry mass related algorithms.

Eq. (13) gives for the effective density:

$$\rho_e = (\rho_f - \rho_w) = \frac{W_S \, 18 \, \mu}{D_Y D_X g} \tag{14}$$

The effective density is the difference between the floc bulk density (ρ_f), and the water density (ρ_w). The water density was calculated from measured salinity and water temperature using the International Equation of State of Sea Water, 1980 (Millero and Poisson, 1981). These values were also used to determine dynamic molecular viscosity. As both salinity and temperature were kept relatively constant throughout the experiments, variations in the floc size and settling velocity will have the greater influence on the effective density of the flocs.

The volume of an ellipsoidal floc (V_f) is given by:

$$V_f = \frac{4 \pi D_Y D_X^2}{3} \tag{15}$$

The interstitial water (V_{iw}) within each floc was calculated by:

$$V_{iw} = 1 - \frac{\rho_e}{\rho_{e\,np}} V_f \tag{16}$$

where $\rho_{e\,np} = \rho_{mo} - \rho_w$; ρ_{mo} is the mean dry density of the primary particles, and $\rho_{e\,np}$ is the mean

effective density for solid (non-porous) aggregates. Estuarine flocs generally have a mineral to organic mass ratio of 90:10, respectively, and a mineral to organic volume ratio of 78:22 (Fennessy, 1994). So, making the assumption that the mineral dry density is 2600 kg m^{-3} and the organic matter having a dry density of 1030 kg m^{-3}; this results in a ρ_{mo} of 2256 kg m^{-3}.

Floc porosity (P_f), which provides an indication to the level of compactness of the floc, was evaluated by taking the ratio of the volume of the floc interstitial water to that of the total floc volume:

$$P_f = \frac{V_{iw}}{V_f} \times 100 \quad (17)$$

Assuming the interstitial fluid density to be equal to ρ_w, the dry floc mass ($M_{f\,dry}$) could be calculated by:

$$M_{f\,dry} = V_f \frac{\rho_e\,\rho_{mo}}{(\rho_{mo} - \rho_w)} \quad (18)$$

An estimation of the fractal dimension, nf, was made using Eq. (7) with the assumption of the primary particle diameter (D_p) as 4 μm, and the empirical coefficient (α') as 0.05. The latter coefficient was calculated from Eq. (7) by using a fractal dimension of two, and then substituting in floc data from the Tamar estuary which was obtained in situ by Fennessy et al. (1994a); from this an average α' value was produced.

To simplify the data interpretation, two sample-group means were generated for each of the floc parameters. Average parameters (with respect to size) from each of the 20 flocs within each sample-group (max20size) are used to illustrate general trends in the data. The average of the four fastest settling flocs present within each sample-group ($max4W_S$) were used to highlight patterns with respect to the maximum settling rates. Both averages were dry mass weighted so as to compensate for variations in aggregate density within each sample-grouping. The validity of the sample means was statistically analysed via a two-sample heteroscedastic *t*-test. This *t*-test type assumes that the variances of both ranges of data are unequal.

7. Results

The data was processed in the manner outlined in the previous section for the sample-groups measured

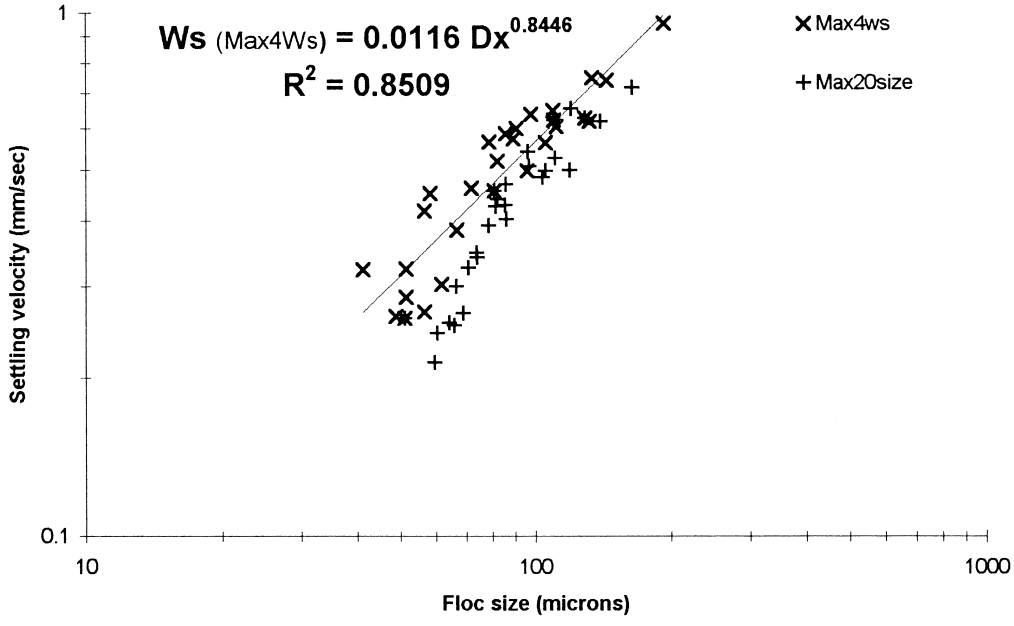

Fig. 2. Variations in settling velocity with floc size at 2 min.

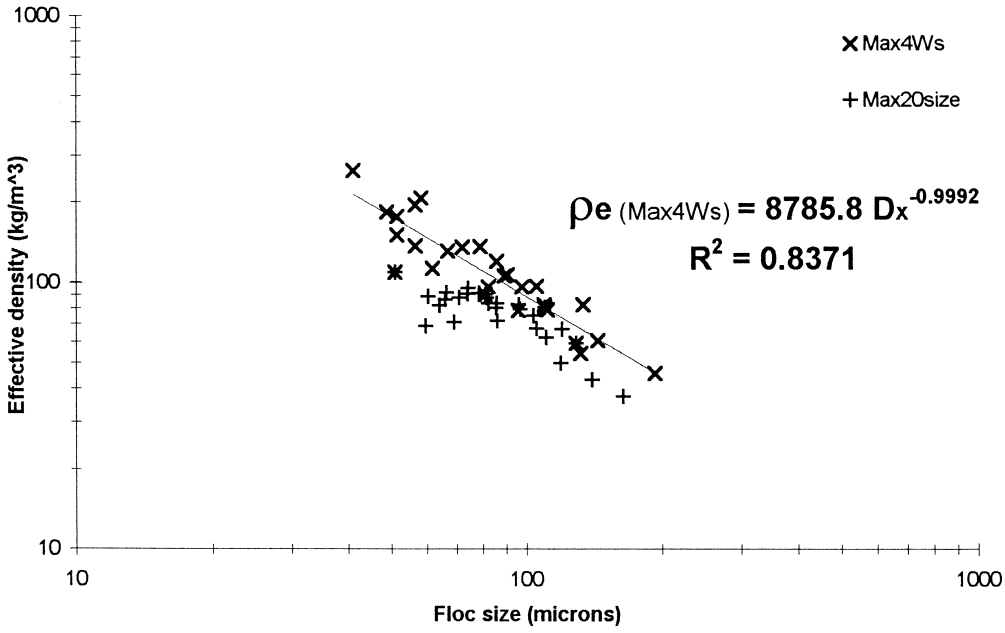

Fig. 3. Variations in calculated effective density with floc size at 2 min.

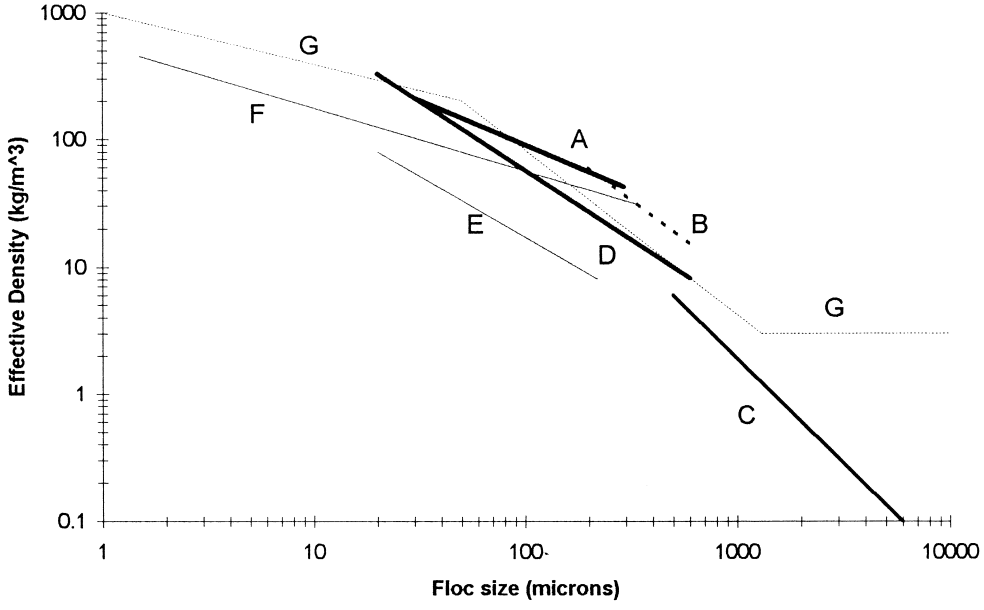

Fig. 4. Comparative results of effective density with floc size. A = this paper (max4W_S at 2 min), B = Al Ani et al. (1991), C = Alldredge and Gotschalk (1988), D = Fennessy et al. (1994a), E = Gibbs (1985), F = McCave (1975), and G = McCave (1984).

at the 2 min-time increment. As previously mentioned, the experimental set-up did not permit the measurement of floc characteristics directly after stirring, but the measurement after 2 min of turbulence decay was deemed to be representative of aggregates produced at their respective shear and

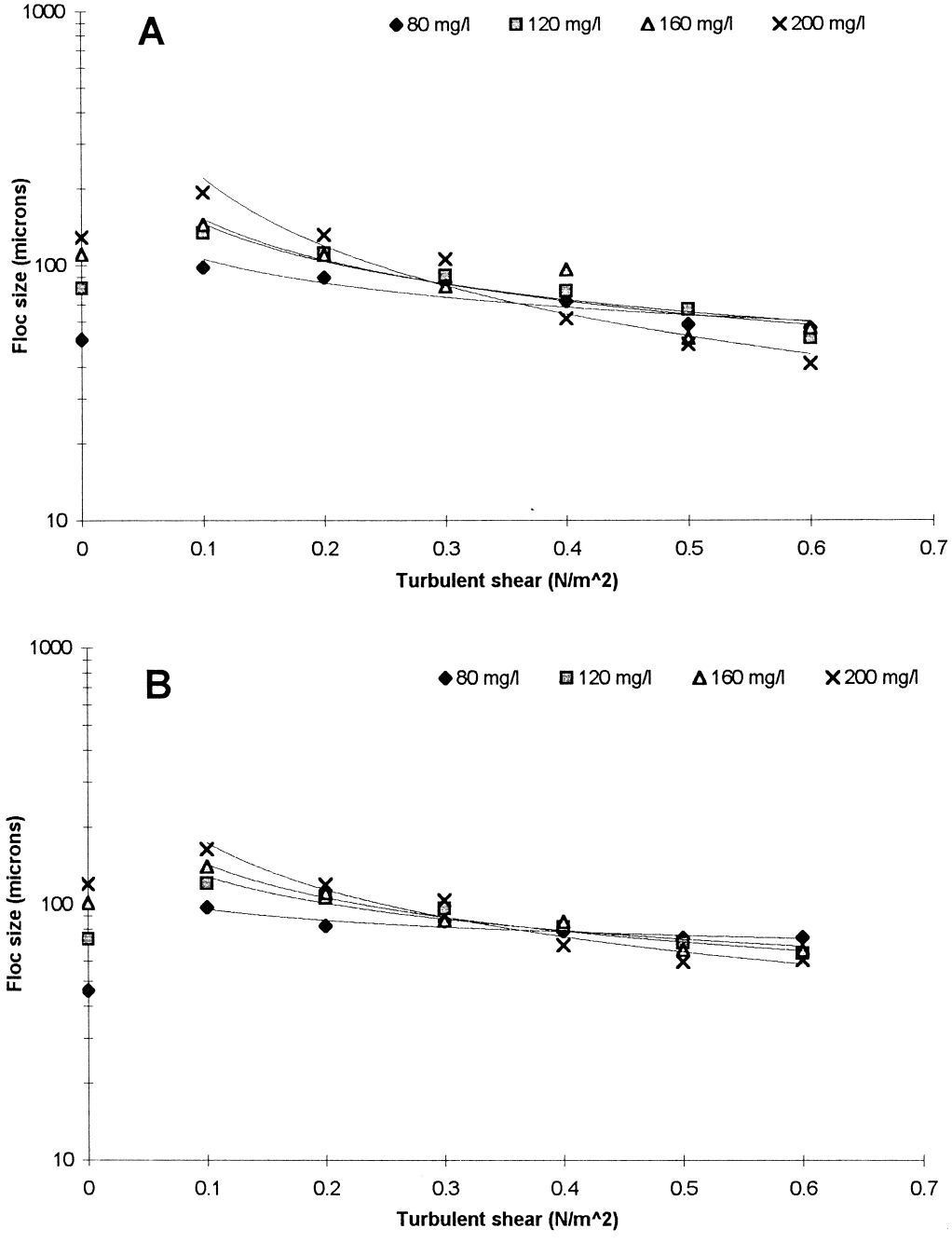

Fig. 5. Variations in max4W_S (A) and max20size (B) floc size over the experimental turbulent shear range, with SPM concentration as a parameter. Power regression lines have been added.

concentration levels. The experiment produced a size range (D_X) of individual flocs from 36.5 to 225 μm. The settling velocity ranged between 0.20 to 1.05 mm s^{-1}, whilst effective density had values from 28 to 286 kg m^{-3}. The statistical *t*-test analysis revealed that the variances were much smaller for the max4W_S mean parameters. However, a comparison between the max20size sample-group means of the 200 mg l^{-1} and 80 mg l^{-1} SPM concentrations (at the same shear stresses) were still found to be significantly different at both the $P < 0.05$ and $P < 0.025$ levels of significance. The max20size and max4W_S averages produced standard deviations ranging between 1.4–3.5 μm and 0.5–2.0 μm, respectively. Therefore, the use of both maximum mean parameters to illustrate flocculation trends was justified.

The mean Reynolds numbers (R_e) for each of the sample-groups is well below 0.5, which is the limit for the use of the Stokes' formula (Ten Brinke, 1993). Consequently, it was thought unnecessary to use the Oseen modification (Oseen, 1927) which compensates for the increased inertia due to faster settling flocs. The flocs had height:width ratios between 0.9 and 1.9, with an experimental average of 1.34:1.

The mean parameters (both types) of floc size against settling velocity for the 2 min sample-group increment have been plotted in Fig. 2. The relationship between settling velocity and floc size indicates that the 2 min flocs produced a large size range with increasing settling velocity values. Effective density data points (Fig. 3) demonstrate a similar pattern to those found in many European tidal estuaries: a large spread in values for the smaller flocs, with a gradual decrease in both spread and effective density as the aggregates increase in size. When comparing the regression line through the max4W_S samples with a variety of other authors studies (Fig. 4), a good comparison can be seen between the data and that collected in situ by INSSEV from previous studies conducted within the Tamar estuary (Fennessy et al., 1994b). The large spread in the remaining trend lines highlights the possible dangers of using data measured by techniques not incorporating the largest flocs. It is clear that the results cannot be represented by a single fractal dimension. Dyer and Manning (1998) detail the pros and cons of a purely fractal-based approach to floc modelling.

The flocs were observed to be elongated in the plane of the mean shear produced by the flow within the annular flume channel. The higher levels of form drag created around the flocs at high shear levels resulted in the formation of long thin 'comet-like' aggregates; only the lower turbulent environments produced more spherically shaped flocs.

Fig. 5A and B show log–linear plots of floc size (max4W_S and max20size, respectively) against shear stress, and with SPM concentration. Power regression lines of the form floc parameter (D_X, W_S or ρ_e) $= f(G)^h$, have been plotted through the data

Table 2
The regression equation coefficients (f and h) and R^2 for Figs. 5–7

	SPM (mg/l)	Max4W_S			Max20size		
		Constant f	Exponent h	R^2	Constant f	Exponent h	R^2
Floc size	80	51.09	−0.32	0.89	63.75	−0.19	0.90
	120	46.22	−0.50	0.92	55.74	−0.37	0.92
	160	43.99	−0.54	0.85	52.46	−0.44	0.96
	200	28.39	−0.89	0.95	35.87	−0.74	0.96
Settling velocity	80	0.39	−0.24	0.85	0.31	−0.22	0.82
	120	0.30	−0.48	0.84	0.24	−0.47	0.81
	160	0.23	−0.61	0.86	0.23	−0.47	0.87
	200	0.18	−0.75	0.90	0.16	−0.69	0.88
Effective density	80	229.97	0.43	0.81	97.74	0.10	0.88
	120	173.86	0.37	0.83	95.05	0.16	0.73
	160	176.46	0.49	0.78	114.95	0.41	0.96
	200	336.17	0.97	0.90	106.92	0.45	0.89

points; however, the zero shear points were not included in the regression analysis as they were taken under different experimental conditions, and are only presented as an indication of those condi-

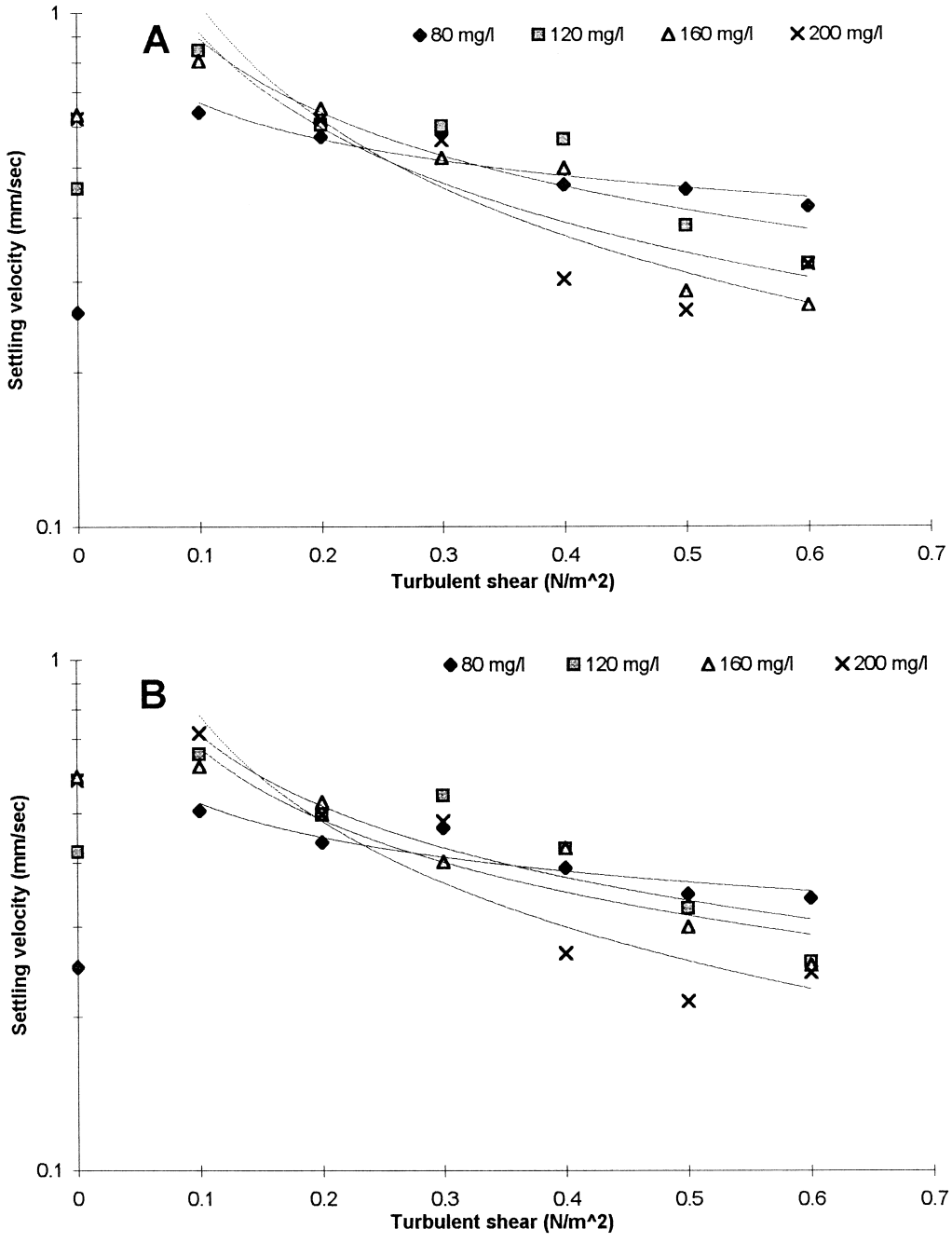

Fig. 6. Variations in max4W_S (A) and max20size (B) settling velocity over the experimental turbulent shear range, with SPM concentration as a parameter. Power regression lines have been added.

tions. A summary of each regression equation coefficients (h and f), together with their R^2 values, is presented in Table 2. The settling velocities (Fig. 6A and B) can be seen to vary through both the shear and concentration levels, in a similar manner to the floc sizes, but with varying magnitudes as a result of

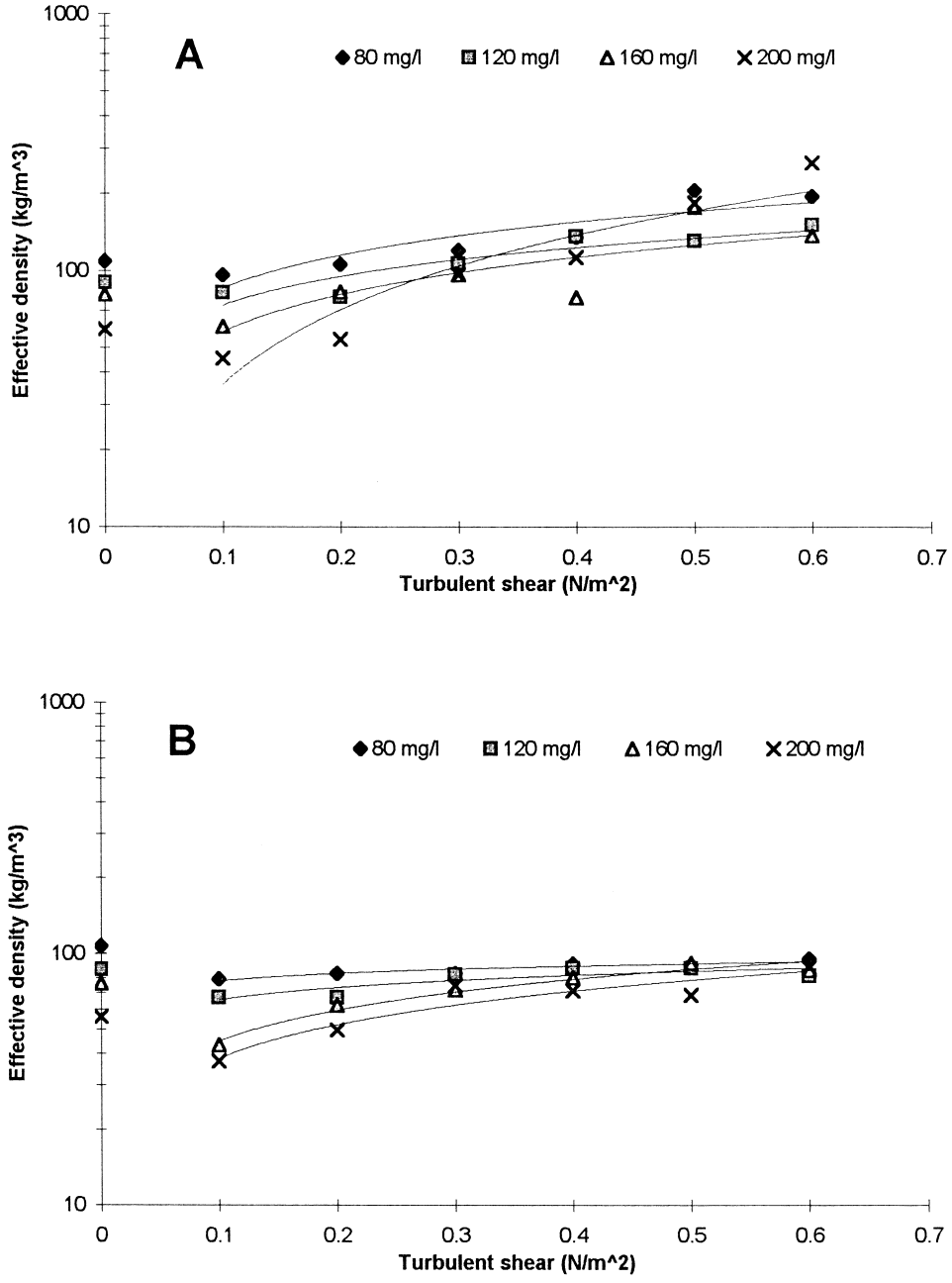

Fig. 7. Variations in max4W_S (A) and max20size (B) floc effective density over the experimental turbulent shear range, with SPM concentration as a parameter. Power regression lines have been added.

altering effective density (Fig. 7A and B). This suggests that the shear has a direct influence on the structural composition of individual flocs.

Computed mean values of aggregate porosity have been plotted against shear stress in Fig. 8, for different SPM concentrations. The algorithms used to

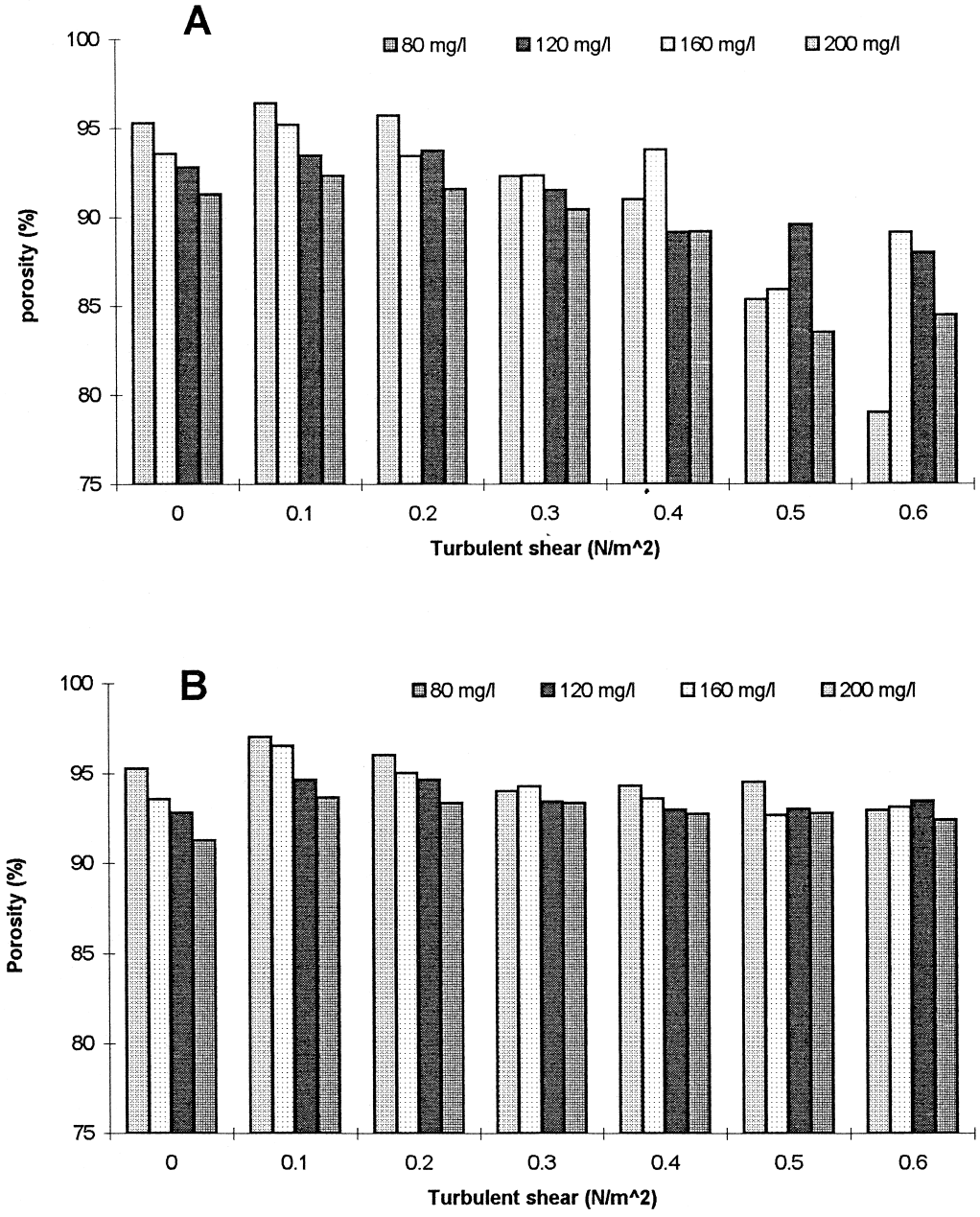

Fig. 8. Histogram of max4W_S (A) and max20size (B) calculated floc porosity over the experimental turbulent shear range, with SPM concentration as a parameter.

determine individual mean floc dry mass, showed that values varied over two orders of magnitude, ranging between 10^{-12} to 10^{-14} kg, and histograms similar to those for aggregate porosity have been plotted in Fig. 9. These parameters revealed some interesting characteristics about the flocs under the

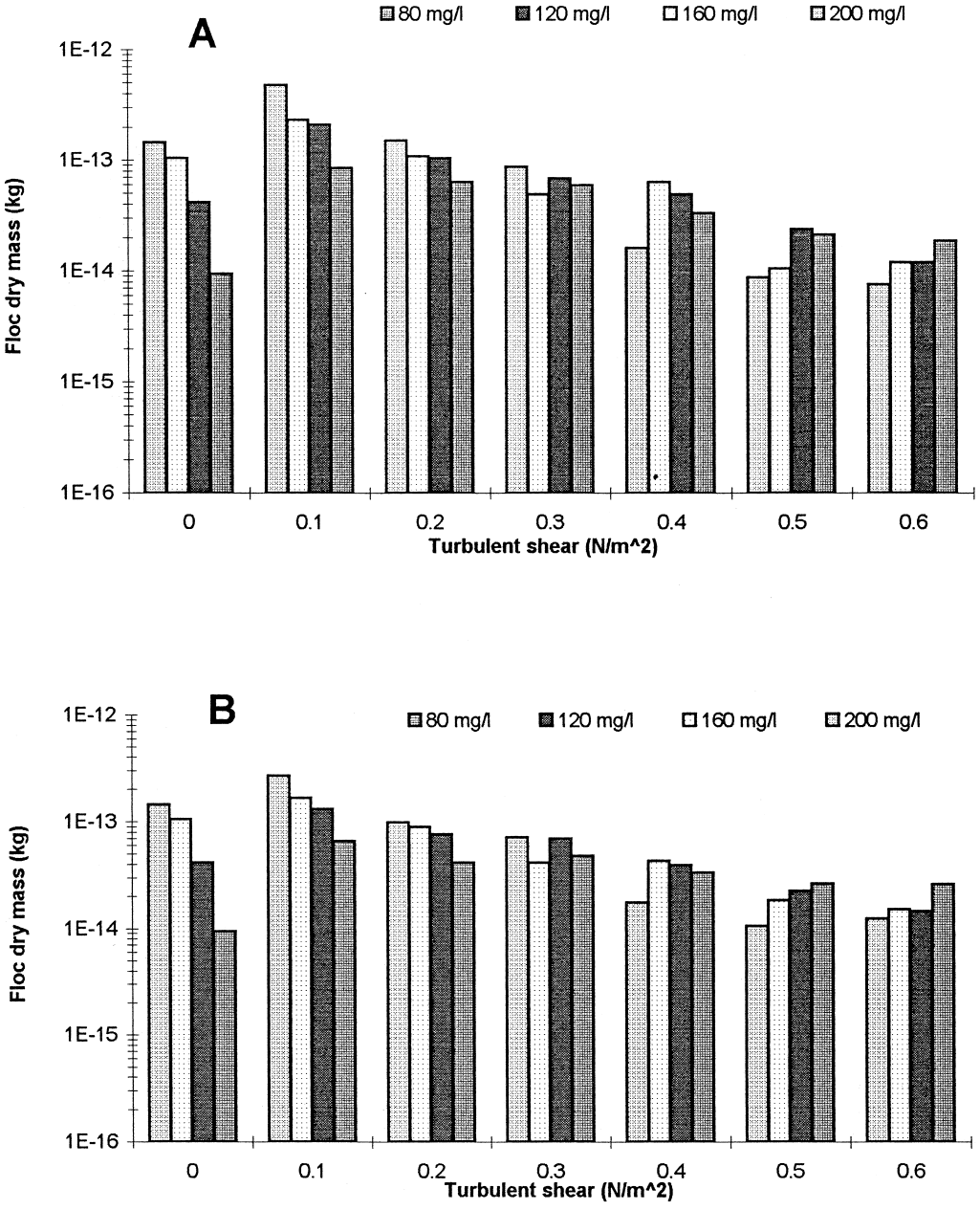

Fig. 9. Histograms of max4W_S (A) and max20size (B) calculated floc porosity over the experimental turbulent shear range, with SPM concentration as a parameter.

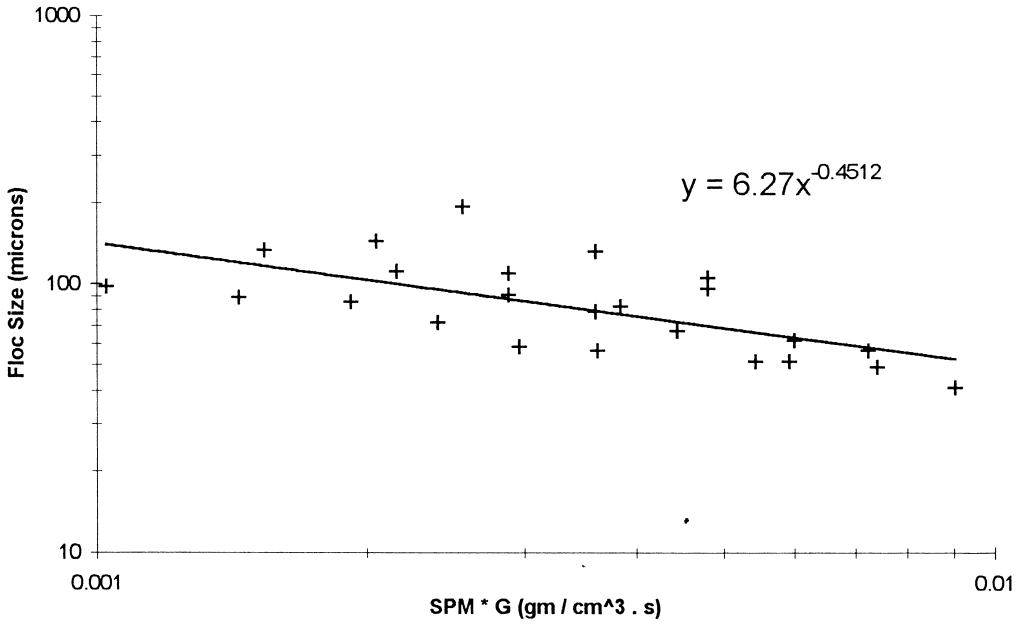

Fig. 10. Variations in floc size (max4W_S only) as a function of the product of suspended particulate matter (SPM) concentration (g/cm^3) and turbulent shear G (s^{-1}).

different environments which will be examined in the next section.

For inter-comparison purposes, three different approaches were used to model the experimental data. Primarily, using the Minitab 10 statistical package to perform a multiple linear regression analysis, it was revealed that only a formula that included the parameters of floc size, SPM concentration and shear stress

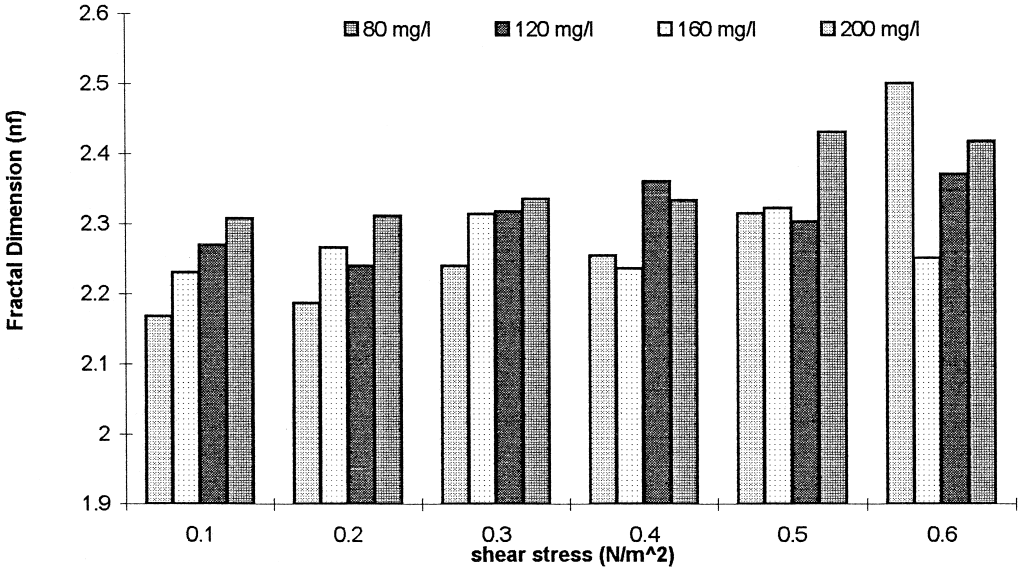

Fig. 11. A histogram of calculated fractal dimension nf (max4W_S only) against turbulent shear, with SPM concentration as a parameter.

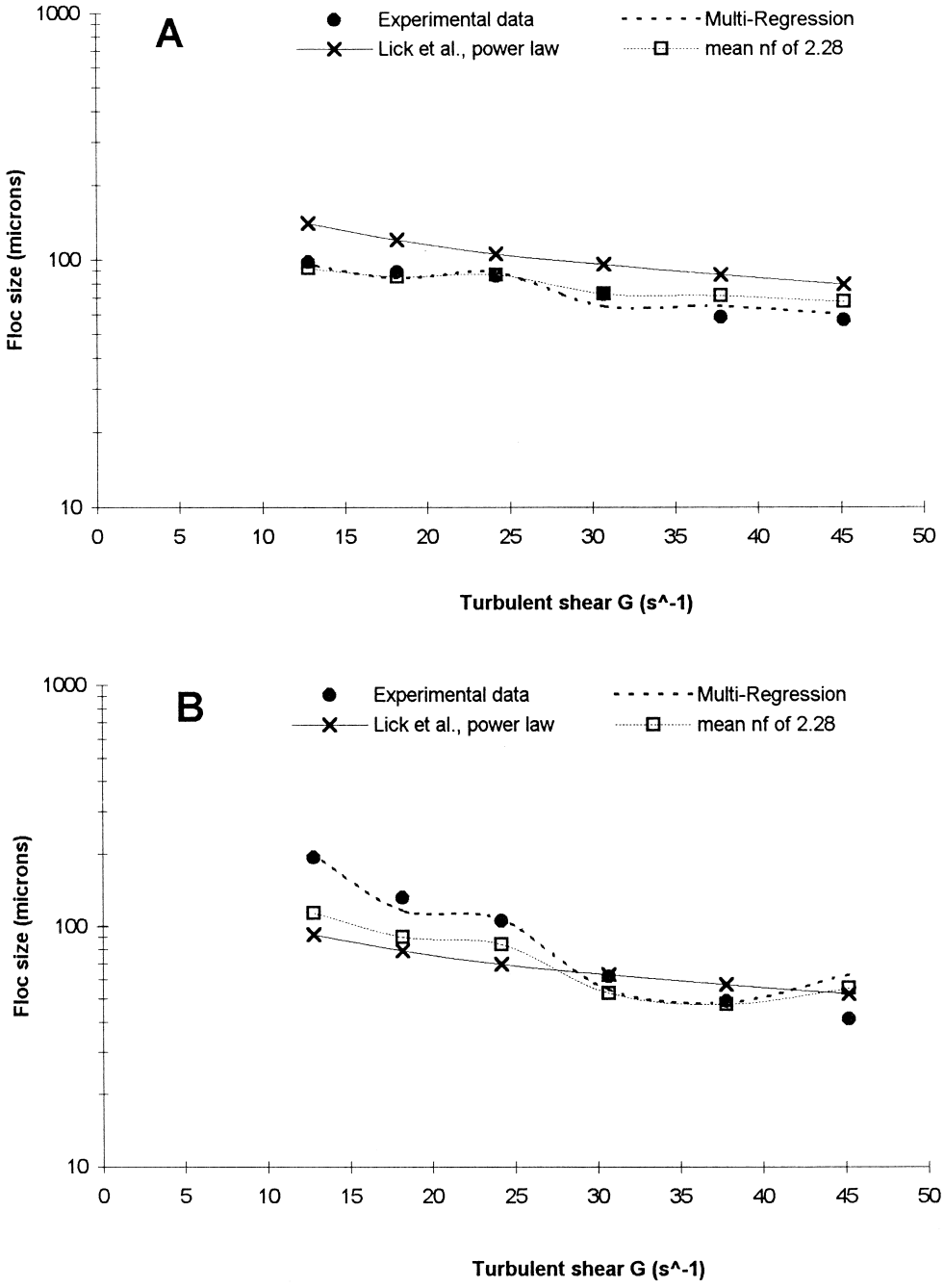

Fig. 12. A comparison of experimental mean floc size ($\max 4W_S$) and values computed by the multiple regression, Power law of Lick et al. (1993) and mean nf of 2.28 approximations, over the experimental shear range ($A = 80$ mg/l and $B = 200$ mg/l).

could accurately represent the variations in settling velocity:

$$W_S = 0.261 - 0.00131\,G - 0.000924\,\mathrm{SPM} + 0.00485\,\mathrm{size}\;D_X \quad \max 4W_S \qquad (19a)$$

$$W_S = 0.301 - 0.00337\,G - 0.000606\,\mathrm{SPM} + 0.00335\,\mathrm{size}\;D_X \quad \max 20\mathrm{size} \qquad (19b)$$

The units for all three algorithm types are: floc size in microns, shear stress (G) in s^{-1}, settling velocity

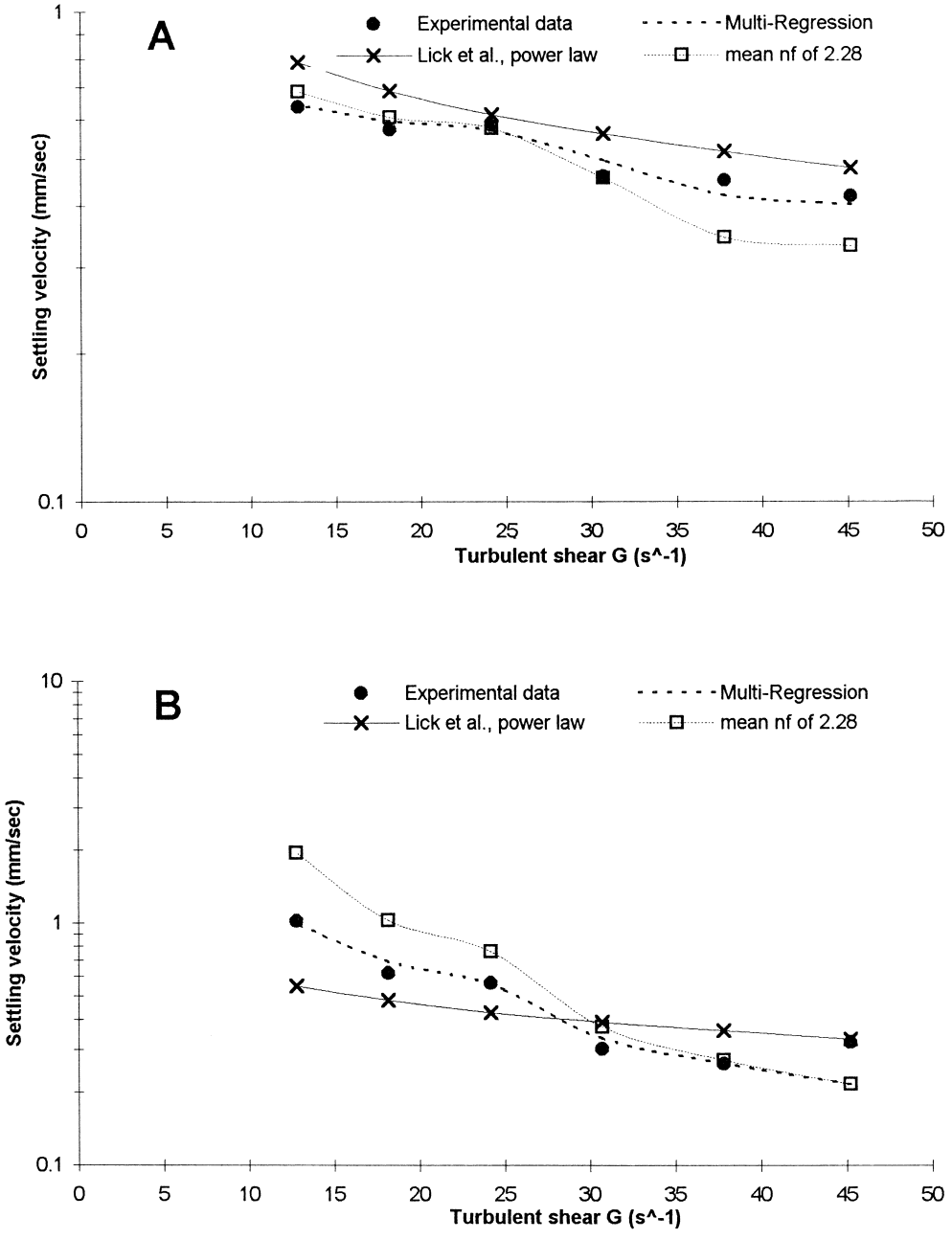

Fig. 13. A comparison of experimental mean settling velocity ($\max 4W_S$)and values computed by the multiple regression, Power law of Lick et al. (1993) and mean nf of 2.28 approximations, over the experimental shear range ($A = 80$ mg/l and $B = 200$ mg/l).

in mm s^{-1} and SPM in mg l^{-1}. The small deviation between the experimental means and those obtained by the multiple regression, is shown by the R^2 values of 0.945 and 0.953 for formulae 19a and 19b, respectively. These formulae can then be rearranged with respect to floc size (i.e., a measured settling velocity is input):

$$D_X = 206.19\,W_S + 0.27\,G + 0.19\,\mathrm{SPM} - 53.80 \quad \max 4W_S \tag{20a}$$

$$D_X = 298.51\,W_S + 1.01\,G + 0.18\,\mathrm{SPM} - 89.85 \quad \max 20\mathrm{size} \tag{20b}$$

It should be noted that this type of multiple regression approach means that the coefficients have dimensions and hence include physical processes. However, in the context of this study, the ability not to be able to arrive at dimensionless coefficients and hence simplify the formulae was of little concern, as this type of formulae highlighted the level of dependence and influence each independent variable had on the resultant dependent variable.

The second algorithm is based on the non-linear formulation used by Lick et al. (1993). A power regression analysis of the floc diameter against the product of the corresponding turbidity and shear stress (Fig. 10), produced the following relationship with respect to floc size:

$$D_X = 6.27(\mathrm{SPM}\,G)^{-0.45} \quad \max 4W_S \tag{21a}$$

$$D_X = 12.61(\mathrm{SPM}\,G)^{-0.37} \quad \max 20\mathrm{size} \tag{21b}$$

The units are the same as the multiple regression model, except SPM which is in g cm^{-3}. Settling velocity can then be approximated as a function of the calculated floc diameter (Gibbs, 1985; Ten Brinke, 1993) to give:

$$W_S = 0.0033\,D_X^{1.137} \quad \max 4W_S \tag{22a}$$

$$W_S = 0.0010\,D_X^{1.352} \quad \max 20\mathrm{size} \tag{22b}$$

The final relationship, computes the fractal dimension from the setting velocities via the Winterwerp formula (Eq. (7)). A histogram illustrating calculated fractal dimensions (nf) for each sample-group are displayed in Fig. 11; a best-fit nf value for the complete experimental range is 2.28. Re-arrangement of Eq. (7) also allows estimation of the floc sizes based on settling velocity data.

The floc size values predicted by each of the three algorithms ($\max 4W_S$ only), are shown graphically for both the 80 and 200 mg l^{-1} SPM concentrations (Fig. 12), and compared with the corresponding ex-

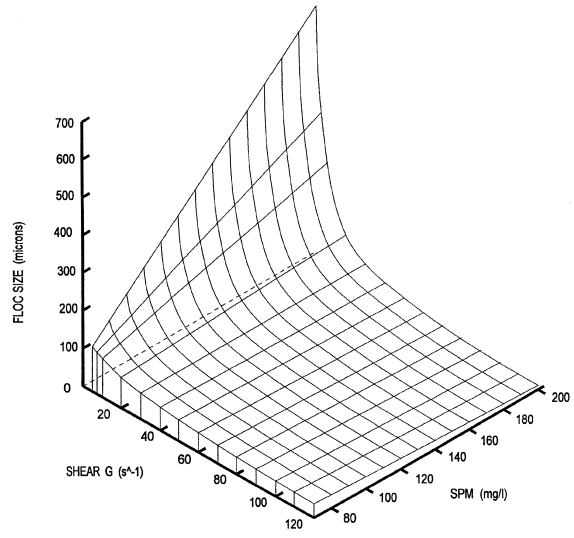

Fig. 14. The relationship between turbidity shear and floc size computed by the multiple regression approximation (equation), using experimental settling velocity values and an extrapolated turbulent shear range; this produces a floc size range beyond those sampled during the experiment. Note the decrease in floc size with increasing shear and SPM concentration.

perimental mean data points. Fig. 13 shows a similar comparison for settling velocity values. The multiple regression appears to approximate the experimental data much more closely than the other two approaches, as one would expect. In Fig. 14, the floc diameters computed by the multiple regression approach has been plotted as a three-dimensional graph against both SPM and shear. The turbulent shear range has been extrapolated (5 to 120 s^{-1}) beyond those used for the actual experiments, for illustrative purposes. There is qualitative agreement with Fig. 1.

8. Discussion

The principle ranges of turbulent shearing used for these experiments, 0.1 to 0.6 N m^{-2} (G = 12.8 to 45.2 s^{-1}), is identified by Van Leussen (1994) as a region of high turbulence which could be expected to occur in the bottom boundary layer during periods of high current velocities. An rms of the gradient in turbulent velocity fluctuations (G) of 0.1 to 1.0 s^{-1} is representative of slack water, but the region between 1.0 and 10 s^{-1} (representative of the mid-water column of an estuary) contributes a great deal to floc growth, as this amount of stirring stimulates the aggregation mechanism of differential settling.

The experimental set-up of the shallow water column within the flume channel, together with the induced shear range used, had a net result of producing flocculation solely by turbulent shear, with a negligible influence of differential settling; this probably accounted for the relatively small sizes of the macro flocs sampled. It is for these reasons, that the maximum floc sizes are probably less than the corresponding Kolmogorov microscale eddy size. Nevertheless, the G values used for the experimental work showed a good correspondence with floc size (Hunt, 1986), i.e., $D_X \propto G^{-m}$, where the exponent m varied between 0.47 and 1.29 for the 80 and 200 mg l^{-1} concentrations, respectively. The flocs measured at the zero shear level are only indicative of those conditions, as a different experimental method had to be used to produce them. The consistently lower size of the aggregates (than those measured at the corresponding 0.1 N m^{-2} rate) can be attributed to a domination by thermal perikinetic flocculation (Brownian motion), which has a much lower collision frequency rate than that due to turbulent shear, and to the probability that equilibrium floc sizes may not have been achieved.

The floc parameters plotted against shear stress (Figs. 5 and 6) showed that at the lowest shear level (0.1 N m^{-2}), there was a distinctive near-linear increase in floc size with increasing SPM concentration; correspondingly, the settling velocities increased. The mean effective density (max20size) of the 200 mg l^{-1} samples (at 0.1 N m^{-2}) was 37 kg m^{-3}, which indicates these flocs are very fragile in nature, and may be subject to settling velocity changes in stratified waters. The formation of aggregates of this type are primarily as a result of the abundance of particulates present within the water column tending to dominate the flocculation process, with the turbulence generally producing constructive particle collisions. The effect diminishes with the increase in shear stress when the turbulence disruption reduces the floc size and increases the density. This process could be seen visually on the monitor screen during data processing; at high shear rates a bi-modal population of primary particles and micro flocs could be visually recognised, and as the turbulent shear was decreased, the percentage of primary particles was seen to drop as they were involved in flocculation.

An important feature highlighted from the data is the cross-over points on the regression lines between shear stresses of about 0.2–0.4 N m^{-2} (Figs. 5 and 6). These mark the shear levels whereby the effect of the increasing turbulent shear on the floc size and settling velocity characteristics, together with the presence of greater amounts of particulates in suspension, causes disruption rather than enhancing the flocculation process. Thus, the higher concentrations result in larger flocs for low shear stresses and the lowest SPM concentration produced the larger mean floc size for the higher shear stress. A similar pattern was observed for the settling velocities.

Extrapolation from the regression lines indicates that for a 200 mg l^{-1} concentration a 1.5 N m^{-2} level of shear would produce a 20 μm maximum floc size, whereas a 19.1 N m^{-2} shear stress is required to produce a similar maximum aggregate size for an 80 mg l^{-1} turbidity level. However, shear stresses of this magnitude would be expected within a typical estuarine water column, so therefore both

an increase in particulate concentration together with shear would be required to produce the smaller maximum floc sizes.

The structural weakness of the large macro flocs can be demonstrated by a comparison of the computed mean aggregate porosity and dry mass (Figs. 8 and 9). As explained earlier, under the high shear environments, small micro flocs are formed, but because the particles are coagulating under high levels of turbulence, the number of voids is minimised; this can be shown by the 80 mg l^{-1} concentration flocs having an average porosity of 78.9% at 0.6 N m^{-2} and a respective mean dry mass of 7.6×10^{-15} kg. These values decrease slightly with increasing SPM at the highest shear stress level. At the more quiescent low shear stresses, the inter-particular collisions are of a sufficient magnitude to allow the particles to readily coagulate, with minimal destructive effects. However, these constructive collisions resulted in the larger macro flocs having a higher porosity (up to 96.4%), and even though their particle dry mass is greater (mean dry mass of 4.78×10^{-13} kg), they are significantly weaker and prone to rapid break-up by a small increase in turbulent shearing. It is reasonable to assume that the strong micro flocs formed under the high shear conditions form the basis of the larger aggregates produced at the lower levels of turbulent energy dissipation.

Even so, for the larger flocs there was a much larger variation in effective density, and this imposes a greater control over the floc settling velocity, as opposed to that of the smaller mean floc size range. These findings on effective density agree with observations made by Fennessy et al. (1994b) over a tidal cycle in the Tamar estuary.

This point emphasises the requirement for simultaneous floc size and settling velocity observations in order to produce semi-empirical flocculation algorithms (especially when the complete size spectrum has been sampled), and hence the need for instruments that are capable of obtaining such data. Algorithms based on the observations of just a single floc characteristic, such as size, carry many risks. This is demonstrated by the large deviation from the experimental settling velocities by those computed via both the Lick et al. (1993) power law, and average fractal dimension value approaches (Figs. 12 and 13).

9. Conclusion

Turbulent shear produced within the water column is recognised as a controlling influence over both flocculation and break-up dynamics. Within an estuarine system, the flocs are thought to be in a quasi-equilibrium state as they are transported between zones of continually changing levels of energy dissipation.

The results from this study showed that increasing turbidity at low shear levels encouraged floc growth. However, the experiment consequently indicated a critical shear (0.35 N m^{-2}), and once this was exceeded, together with a simultaneous increase in concentration in suspension, disruption causing aggregate break-up was created, as opposed to enhancement of the flocculation process. At shears up to 0.35 N m^{-2}, the largest size and settling velocity flocs were produced at high concentrations, whereas above 0.35 N m^{-2} disruption caused smaller flocs at higher concentrations. This observation may vary for different suspensions depending upon the mineralogy and biological properties of the individual particles.

A limitation of previous estuarine sediment flux models could be attributed to the use of empirically derived algorithms that approximated aggregate settling velocity in a turbulent flow, either based on a median settling value, or as a function of floc diameter. The use of an unintrusive video camera to measure the aggregate properties facilitates an examination of the potential variations in floc structure throughout the imposed environmental conditions. From the results obtained, it can be seen that turbulent shear has a significant influence over both the porosity and strength of an aggregate formed, and consequently the effective density.

The low effective density macro flocs formed at the 0.1 N m^{-2} shear stress were of considerably high porosity, and hence deemed very fragile. Due to the fact that the stronger (low porosity) micro flocs formed under the higher shear environment had a much greater spread in effective densities, it is therefore plausible that some may survive as the shear level in the flume decreases during a run, and are re-suspended to form the basis of the macro flocs, as advocated in the classic order of aggregation theory.

So, although shear can be seen to have a control over floc size, algorithms that do not take into

account effective density variations (i.e., are not formulated from simultaneous settling velocity and floc size measurements data) will produce an unrealistic representation. This hypothesis, is perfectly illustrated by the comparison of the multi-regressional model, and the type advocated by Lick et al. (1993). Similar over simplifications, such as the use of an average fractal dimension value, may inevitably lead to either under or over estimates of mass settling flux.

Acknowledgements

The authors would like to thank Mike Fennessy, Malcolm Christie and the Institute of Marine Studies technicians, for their assistance during the initial development of the flume instrumentation. The work was partly funded by EC MAST III contracts MAS3/CT95.0022 INTRMUD and MAS3-CT97-0082 COSINUS.

References

Al Ani, S., Dyer, K.R., Huntley, D.A., 1991. Measurement of the influence of salinity on floc density and strength. Geo-Mar. Lett. 11, 154–158.

Alldredge, A.L., Gotschalk, C., 1988. In situ settling behaviour of marine snow. Limnol. Oceanogr. 33, 339–351.

Allen, T., 1975. Particle size measurement. Chapman & Hall, London, 454 pp.

Argaman, Y., Kaufman, W.J., 1970. Turbulence and flocculation. J. Sanitary Eng. ASCE 96, 223–241.

Ayesa, E., Margeli, M.T., Florez, J., Garcia-Heras, J.L., 1992. Estimation of break-up and aggregation coefficients in flocculation by a new algorithm. Chem. Eng. Sci. 46 (1), 39–48.

Bale, A.J., Morris, A.W., 1987. In situ measurement of particle size in estuarine waters. Estuarine Coastal Shelf Sci. 24, 253–263.

Burban, P.Y., 1987. The flocculation of fine-grained sediments in estuarine waters. MSc. thesis, Dep. of Mech. Eng. Univ. of Calif., Santa Barbara, USA.

Burban, P.-Y., Lick, W., Lick, J., 1989. The flocculation of fine-grained sediments in estuarine waters. J. Geophys. Res. 94 (C6), 8323–8330.

Burban, P.-Y., Xu, Y.-J., McNeil, J., Lick, W., 1990. Settling speeds of flocs in fresh water and seawater. J. Geophys. Res. 95 (C10), 18213–18220.

Chow, V.T., 1959. Open Channel Hydraulics. McGraw-Hill, New York.

Delo, E.A., 1988. Estuarine muds manual. Hydraulics Research, Wallingford. Report No. SR164, pp. 23–26.

Dyer, K.R., 1986. Coastal and Estuarine Sediment Dynamics. Wiley, Chichester, 342 pp.

Dyer, K.R., 1989. Sediment processes in estuaries: future research requirements. J. Geophys. Res. 94 (C10), 14327–14339.

Dyer, K.R., Manning, A.J., 1998. Observation of the size, settling velocity and effective density of flocs, and their fractal dimensions. J. Sea Res., in press.

Eisma, D., Boon, J., Groenewegen, R., Ittekkot, V., Kalf, J., Mook, W.G., 1983. Observations on macro-aggregates, particle size and organic composition of suspended matter in the Ems estuary. Mitt. Geol.-Palaontol. Inst. niv. Hamburg, SCOPE/UNEP Sonderbereich 55, 295–314.

Eisma, D., Schuhmacher, T., Boekel, H., Van Heerwaarden, J., Franken, H., Lann, M., Vaars, A., Eijgenraam, F., Kalf, J., 1990. A camera and image analysis system for in situ observation of flocs in natural waters. Neth. J. Sea Res. 27, 43–56.

Eisma, D., Bernard, P., Cadee, G.C., Ittekkot, V., Kalf, J., Laane, R., Martin, J.M., Mook, W.G., Van Put, A., Schuhmacher, T., 1991. Suspended matter particle size in some west European estuaries. Neth. J. Sea Res. 28 (3), 193–220.

Fennessy, M.J., 1994. Development and testing of an instrument to measure estuarine floc size and settling velocity in situ. PhD Thesis. University of Plymouth, 128 pp.

Fennessy, M.J., Dyer, K.R., 1996. Floc population characteristics measured with INSSEV during the Elbe estuary intercalibration experiment. J. Sea Res. 36 (1–2), 55–62.

Fennessy, M.J., Dyer, K.R., Huntley, D.A., 1994a. INSSEV: an instrument to measure the size and settling velocity of flocs in situ. Mar. Geol. 117, 107–117.

Fennessy, M.J., Dyer, K.R., Huntley, D.A., 1994b. Size and settling velocity distributions of flocs in the Tamar Estuary during a tidal cycle. Neth. J. Aquat. Ecol. 28, 275–282.

Fennessy, M.J., Dyer, K.R., Huntley, D.A., Bale, A.J., 1997. Estimation of settling flux spectra in estuaries using INSSEV. Proc. INTERCOH'94, Wallingford, England. Wiley, Chichester, pp. 87–104.

Fitzpatrick, F., 1991. Studies of sediments in a tidal environment. PhD Thesis. Department of Geological Sciences, University of Plymouth, 221 pp.

Gibbs, R.J., 1983. Coagulation rates of clay minerals and natural sediments. J. Sed. Petrol. 53 (4), 1193–1203.

Gibbs, R.J., 1985. Estuarine flocs: their size settling velocity and density. J. Geophys. Res. 90 (C2), 3249–3251.

Gibbs, R.J., Konwar, L.N., 1983. Sampling of mineral flocs using Niskin bottles. Environ. Sci. Technol. 17 (6), 374–375.

Hill, P.S., 1996. Sectional and discrete representations of floc breakage in agitated suspensions. Deep-Sea Res. 43, 679–702.

Hunt, J.R., 1986. Particle aggregate break-up by fluid shear. In: Mehta, A.J. (Ed.), Estuarine Cohesive Sediment Dynamics. Springer, Berlin, pp. 85–109.

Kolmogorov, A.N., 1941a. The local structure of turbulence in incompressible viscous fluid for very large Reynolds numbers. C.R. Acad. Sci. URSS 30, 301.

Kolmogorov, A.N., 1941b. Dissipation of energy in locally isotropic turbulence. C.R. Acad. Sci. URSS 32, 16.

Kranenburg, C., 1994. The fractal structure of cohesive sediment aggregates. Estuarine Coastal Shelf Sci. 39, 451–460.

Krone, R.B., 1963. A study of rheological properties of estuarial sediments. Hyd. Eng. Lab. and Sanitary Eng. Lab., University of California, Berkeley, Report No. 63–68.

Krone, R.B., 1986. The significance of aggregate properties to transport processes. In: Mehta, A.J. (Ed.), Estuarine Cohesive Sediment Dynamics. Springer, Berlin, pp. 66–84.

Lick, W., 1994. Modelling the transport of sediment and hydrophobic contaminants in surface waters. US/Israel Workshop on monitoring and modelling water quality, May 8–13, 1994. Haifa, Israel.

Lick, W., Huang, H., Jepsen, R., 1993. Flocculation of fine-grained sediments due to differential settling. J. Geophys. Res. 98 (C6), 10279–10288.

Manning, A.J., 1996. A laboratory study to examine the response of fine cohesive sediment suspensions to turbulent shearing. MSc. Thesis. Institute of Marine Studies, University of Plymouth, 86 pp.

Manning, A.J., Fennessy, M.J., 1997. INSSEV (In Situ Settling Velocity instrument)—1.3: Operator Manual. Institute of Marine Studies, University of Plymouth, 25 pp.

McCave, I.N., 1975. Vertical flux of particles in the ocean. Deep-Sea Res. 22, 491–502.

McCave, I.N., 1984. Size spectra and aggregation of suspended particles in the deep ocean. Deep-Sea Res. 31, 329–352.

Mehta, A.J., Partheniades, E., 1975. An investigation of the depositional properties of flocculated fine sediment. J. Hydrol. Res. 92 (C13), 361–381.

Mehta, A.J., Lott, J.W., 1987. Sorting of fine sediment during deposition. Proc. Specialty Conf. Advances in Understanding Coastal Sediment Processes. Am. Soc. Civ. Eng., New York, pp. 348–362.

Millero, F.J., Poisson, A., 1981. International one-atmosphere equation of state seawater. Deep-sea Res. 28 (A), 625–629.

Oseen, C.W., 1927. Neuere methoden und ergebnisse. Hydrodynamik. Akad Verlagsges, Leipzig.

Owen, M.W., 1971. The effects of turbulence on the settling velocity of silt flocs. Proc. 14th Cong. Int. Assoc. Hydraul. Res. Paris, pp. D4-1–D4-6.

Pandya, J.D., Spielman, L.A., 1982. Floc break-up in agitated suspensions: theory and data processing strategy. J. Colloid Interface Sci. 90, 517–531.

Parker, D.S., Kaufman, W.J., Jenkins, D., 1972. Floc break-up in turbulent flocculation processes. J. Sanitary Eng. Div. Proc. Am. Soc. Civil Eng. 98 (SA1), 79–97.

Partheniades, E., 1965. Erosion and deposition of cohesive soils. J. Hydr. Div. Proc. Am. Soc. Civ. Eng. 98, 79–99.

Stolzenbach, K.D., Elimelich, M., 1994. The effect of density on collisions between sinking particles: implications for particle aggregation in the ocean. J. Deep-Sea Res. I 41 (3), 469–483.

Tambo, N., Watanabe, Y., 1979. Physical characteristics of flocs: I. The floc density function and aluminium floc. Water Res. 13, 409–419.

Ten Brinke, W.B.M., 1993. The impact of biological factors on the deposition of fine grained sediment in the Oosterschelde (The Netherlands). PhD Thesis, University of Utrecht, The Netherlands, 252 pp.

Tsai, C.H., Iacobellis, S., Lick, W., 1987. Flocculation of fine-grained sediments due to a uniform shear stress. J. Great Lakes Res. 13, 135–146.

Van Leussen, W., 1988. Aggregation of particles, settling velocity of mud flocs: a review. In: Dronkers, J., van Leussen, W. (Eds.), Physical Processes in Estuaries. Springer, Berlin, pp. 347–403.

Van Leussen, W., 1994. Estuarine macroflocs and their role in fine-grained sediment transport. PhD Thesis, University of Utrecht, The Netherlands, 488 pp.

Van Leussen, W., Cornelisse, J.M., 1994. The determination of the sizes and settling velocities of estuarine flocs by an underwater video system. Neth. J. Sea Res. 31 (3), 231–241.

Winterwerp, J.C., 1997. A simple model for turbulence induced flocculation of cohesive sediment. J. Hydraulic Res., IAHR.